

# Application of a DFB fibre laser temperature sensor for characterizing pump induced temperature distributions along another DFB fibre laser

O. Hadeler and M. N. Zervas

Optoelectronics Research Centre, University of Southampton,  
Southampton SO17 1BJ, UK,  
Phone +44 (0)23 8059 3141, Fax +44 (0)23 8059 3142, oh@orc.soton.ac.uk

## ABSTRACT

We demonstrate a novel application for DFB fibre laser temperature sensors, i.e. characterization of the pump induced temperature distribution along another DFB fibre laser, with high temperature and spatial resolution. This provides valuable information for improving DFB fibre laser performance.

## 1. INTRODUCTION

Single mode, single polarisation distributed feedback (DFB) fibre lasers are attractive devices for telecommunication applications.<sup>1,2</sup> Dual polarisation DFB fibre lasers have been used as polarimetric pressure, strain, and temperature sensors.<sup>3,4</sup> DFB fibre lasers consist of a  $\pi/2$ -phase-shifted Bragg grating written into rare-earth doped fibre. The emitted light has a narrow linewidth of the order of tens of kHz. The output power of  $\text{Er}^{3+} : \text{Yb}^{3+}$ -doped DFB fibre lasers can be as high as 20 mW when pumped with  $\sim 150$  mW in the 980 nm band.<sup>2</sup> However, when pumped around 980 nm a considerable amount of heat is generated inside the  $\text{Er}^{3+} : \text{Yb}^{3+}$ -doped fibre which leads to two detrimental effects: an increase of the lasing wavelength due to the overall temperature rise and a drop in output power due to grating chirp induced by the non-uniform temperature distribution along the DFB fibre laser.<sup>5</sup> Therefore, measuring the temperature distribution along DFB fibre lasers could provide valuable understanding for improving laser designs with the aim to increase the output power and reduce the wavelength shift. The temperature distribution could, in principle, be measured with a small thermocouple. However, in a previous experiment we have developed a polarimetric DFB fibre laser temperature sensor with an accuracy of  $\pm 0.04^\circ\text{C}$ ,<sup>4</sup> a factor of two better than many commercial thermocouples. Furthermore, its spatial resolution is given by the mode distribution inside the fibre, i.e.  $\approx \pm 2.5$  mm along the fibre axis and  $\pm 4.5$   $\mu\text{m}$  perpendicular to the fibre axis.<sup>4,6</sup>

In this paper we present a novel application for this DFB fibre laser temperature sensor: characterizing the temperature distribution along another DFB fibre laser with a high spatial and temperature resolution. This information is then used to show possible routes to improve the performance of DFB fibre lasers.

## 2. THEORY

The heat inside the  $\text{Er}^{3+} : \text{Yb}^{3+}$ -doped fibre is generated by the nonradiative decay from the pump level to the upper laser level when pumped at 980 nm.<sup>7</sup> Because the heat transfer along the fibre is impeded by the low thermal conductivity of silica the heat distribution along the fibre is proportional to the distribution of the absorbed pump power,<sup>8</sup> which is expected to be a superposition of the exponential pump power decay along the fibre and the intensity profile of the lasing mode. The latter follows from the laser rate equations<sup>9</sup> which show that the number of absorbed pump photons per unit time at a given position inside the laser is proportional to the intensity of the lasing mode at this particular position. Heat transfer theory shows that the temperature at the fibre surface is proportional to temperature inside the  $\text{Er}^{3+} : \text{Yb}^{3+}$ -doped fibre:<sup>8,10</sup>

$$\Delta T(r) = \frac{\eta P_v s^2}{2bh} - \frac{\eta P_v s^2}{2k} \ln\left(\frac{r}{b}\right), \quad (1)$$

where  $r$  is the radial distance from the centre of the fibre,  $\eta$  is the fraction of pump power turned into heat,  $P_v$  is the absorbed pump power per unit volume,  $s$  is the radius of the absorption boundary inside the fibre,  $b$  is the outer radius of the fibre,  $h$  and  $k$  are the heat transfer coefficient from the fibre to the surrounding medium and the thermal conductivity of the fibre, respectively.

### 3. EXPERIMENTAL ARRANGEMENT

The experimental arrangement for measuring temperature profiles along DFB fibre lasers is shown in Fig. 1. The DFB fibre laser subject to the temperature distribution measurement ( $DFB_I$ ) was pumped by a master oscillator power amplifier (MOPA) whose wavelength could be tuned between 971 nm and 980 nm. This tuneability allowed thermal effects to be studied at pump wavelengths with different absorption coefficients of the fibre. The light from the MOPA was coupled into the 980 nm input of a four port WDM. The pump intensity could be adjusted with a variable attenuator positioned between the MOPA and the fibre launch optics. A maximum pump power of  $\approx 130$  mW was incident on  $DFB_I$ . The left hand output of  $DFB_I$  was detected with an optical spectrum analyser. At the fourth port of the WDM a small fraction of the pump light could be detected to monitor the pump wavelength and pump power. The  $\pi/2$ -phase shift of  $DFB_I$  was positioned asymmetrically at  $\approx 21$  mm of the 50 mm long DFB fibre laser, so the laser output was predominantly towards the left.<sup>2</sup>  $DFB_I$  was either placed on a medium density fibre board (MDF) with low thermal conductivity or an aluminium block with high thermal conductivity.

The polarimetric DFB fibre laser temperature sensor<sup>4</sup> ( $DFB_S$ ) was pumped at 1480 nm. Its polarisation beat frequency was measured with an RF spectrum analyser. The temperature dependence of the beat frequency was  $-0.87$  MHz/ $^{\circ}$ C.  $DFB_S$  was placed perpendicular across  $DFB_I$  and was moved along the axis of the latter with a manual translation stage in steps of 2–4 mm. The surface temperature distribution along  $DFB_I$  was determined by measuring the polarisation beat frequency difference  $\Delta\nu$  of  $DFB_S$  between the unpumped and pumped state of  $DFB_I$ . The crossing point of the two lasers was adjusted so it coincided with the position of the phase shift of  $DFB_S$ , the position most sensitive to temperature changes. A small polystyrene cube was placed on the crossing point of the two lasers to achieve good thermal contact between the lasers while keeping any influence on the two lasers to a minimum. The two lasers were covered by a polystyrene box in order to prevent unwanted airflows and associated temperature fluctuations.

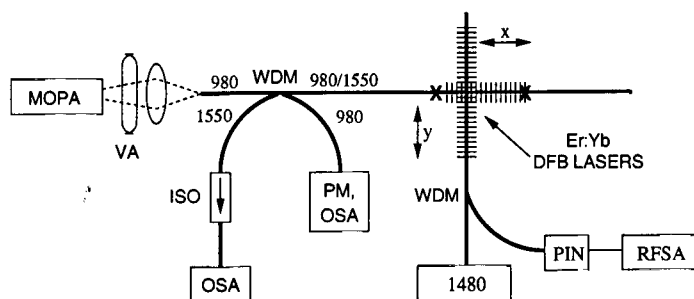


**Figure 1.** Experimental arrangement to measure temperature distribution along a DFB fibre laser ( $DFB_I$ ) pumped at different wavelengths between 971–980 nm. The DFB fibre laser temperature sensor ( $DFB_S$ ) is placed perpendicular across  $DFB_I$ . The grating chirp of  $DFB_I$  could be characterized at the right hand output of the laser. MOPA = master oscillator power amplifier, VA = variable attenuator, WDM = wavelength division multiplexer, PM = optical power meter, OSA = optical spectrum analyser, 1480 = 1480 nm pump diode, PIN = photo diode, RFS = RF spectrum analyser.

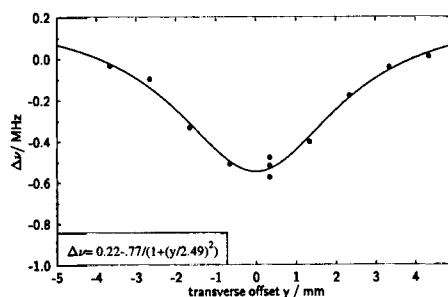


**Figure 2.** Polarisation beat frequency change of the DFB fibre laser temperature sensor as a function of the distance between its phase shift and its crossing point with the heated  $DFB_I$ . The FWHM of the Lorentzian curve is 5 mm which defines the spatial resolution of the sensor along its fibre axis.

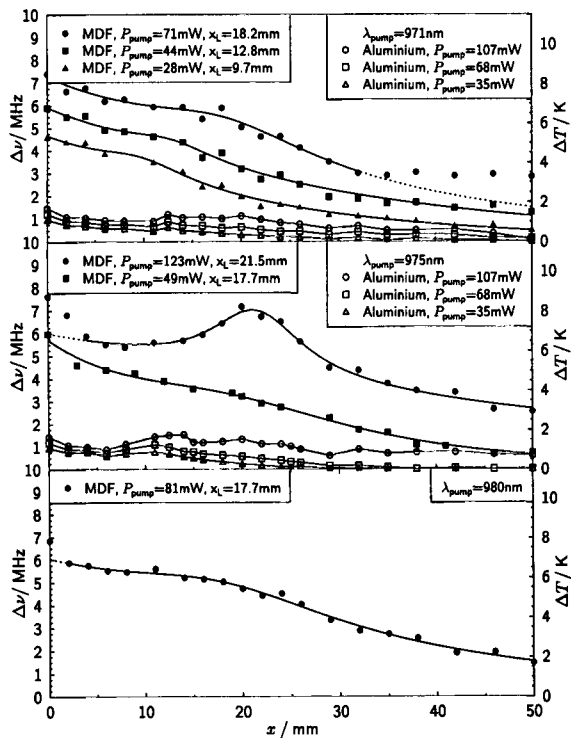


**Figure 3.** Beat frequency shift and apparent surface temperature distribution along DFB fibre laser as a function of pump power and wavelength when placed on MDF board or aluminium. The position of the peak of the Lorentzian curve is denoted by  $x_L$ .

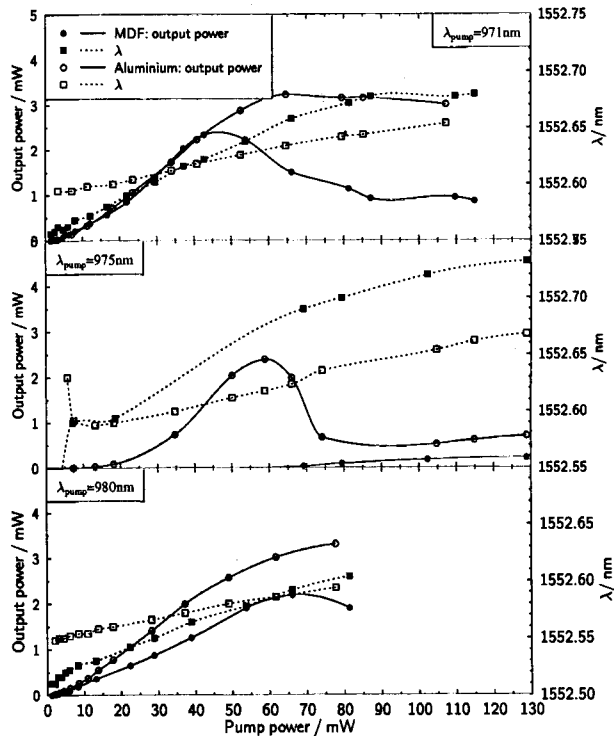


**Figure 4.** DFB fibre laser output power and wavelength as a function of pump power and wavelength when placed on MDF board or aluminium.

#### 4. RESULTS

Fig. 2 shows the temperature sensitivity of DFB<sub>S</sub> as a function of the distance between its phase shift and the crossing point with the heated DFB<sub>I</sub>. The FWHM of the fitted Lorentzian curve was 5 mm, which defines the spatial resolution of the DFB fibre laser temperature sensor along its fibre axis. Fig. 3 shows the temperature induced beat frequency shift  $\Delta\nu$  of DFB<sub>S</sub> as function of position along DFB<sub>I</sub> for different pump power, pump wavelengths, and placed on different materials. DFB<sub>I</sub> was pumped at the absorption peak at 975 nm and on either side of the peak at 971 nm and 980 nm. When DFB<sub>I</sub> was placed on MDF board with a low thermal conductivity significant pump induced temperature changes were observed. The lines represent best fits of a superposition of an exponential pump power decay and a Lorentzian intensity profile of the laser mode. When pumped with 123 mW at 975 nm the temperature distribution was dominated by a Lorentzian peak, i.e. most of the heat was generated in the region where the laser intensity was highest. This in turn would cause considerable chirp of the DFB grating reducing the laser output power. In fact, it can be seen from Fig. 4 that the output power of DFB<sub>I</sub> in this case was only  $\approx 250 \mu\text{W}$  compared to  $> 1 \text{ mW}$  when pumped at 971 nm and 980 nm, where the Lorentzian peaks were less pronounced. It is therefore beneficial not to pump the DFB laser at the peak of the pump absorption although the pump absorption is smaller. It can be observed that the peak position  $x_L$  of the Lorentzian, and therefore the intensity distribution of the laser mode, depended on the pump power at 971 nm. A possible explanation is that at low pump power most of the pump was absorbed near the pump input end. As a result of the temperature induced chirp the  $\pi/2$ -phase shift effectively moved towards the left. When the pump power was increased the ground state of the active ions was bleached and the pump light penetrated further into the grating, pushing the phase shift and the laser intensity distribution further inside the grating towards the original position of the phase shift. However, the output power of DFB<sub>I</sub> decreased after reaching a maximum at a pump power of  $\approx 44 \text{ mW}$  because of temperature induced chirp. Placing DFB<sub>I</sub> on aluminium with a high thermal conductivity reduced the

overall surface temperature significantly and, more importantly, the temperature distribution levelled off, thereby reducing the temperature induced chirp along DFB<sub>I</sub> (see Fig. 3). The reduced temperature rise manifests itself in a smaller pump power dependence of the laser wavelength, shown in Fig. 4. Because the grating chirp was reduced, the output power of DFB<sub>I</sub> increased. However, it can be seen in Fig. 4 that the thermal conductivity of aluminium is not sufficient to prevent temperature induced chirp along the grating when DFB<sub>I</sub> is pumped at high power at 975 nm. The corresponding temperature profile also shows significant non-uniformities along the DFB fibre laser.

## 5. CONCLUSION

In conclusion, we have demonstrated a novel application of a polarimetric DFB fibre laser temperature sensor. The sensor was used to characterize the pump induced temperature distribution along another DFB fibre laser. Significant temperature variations were observed along the DFB fibre laser which depended on pump wavelength, pump power and the material on which the laser was placed. Knowledge of this temperature distribution provides valuable information to improve laser cavity design and laser performance, i.e. increase its output power and reduce wavelength shifts. A direct measurement of the effects of packaging materials on the performance of DFB fibre lasers was presented.

The authors would like to thank M. Ibsen for fabricating the DFB fibre lasers.

## REFERENCES

1. J. Hübner, P. Varming, and M. Kristensen, "Five wavelength DFB fibre laser source for WDM systems," *Electr. Lett.*, vol. 33, no. 2, pp. 139–140, 1997
2. M. Ibsen, E. Rønnekleiv, G. J. Cowle, M. O. Berendt, O. Hadeler, M. N. Zervas, and R. I. Laming, "Robust high power (> 20 mW) all-fibre DFB lasers with unidirectional and truly single polarisation outputs", in *Conf. on Lasers and Electro-Optics 1999*, (Optical Society of America, Washington DC, 1999), paper CWE4
3. J. T. Kringlebotn, W. H. Loh, and R. I. Laming, "Polarimetric Er<sup>3+</sup>-doped fiber distributed-feedback laser sensor for differential pressure and force measurements," *Opt. Lett.*, vol. 21, no. 22, pp. 1869–1871, 1996
4. O. Hadeler, E. Rønnekleiv, M. Ibsen, and R. I. Laming, "Polarimetric distributed feedback fiber laser sensor for simultaneous strain and temperature measurements", *Appl. Opt.*, vol. 38, no. 10 pp. 1953–1958, 1999
5. L. Dong, W. H. Loh, J. E. Caplen, and J. D. Minelly, "Efficient single-frequency fiber lasers with novel photosensitive Er/Yb optical fibers", *Opt. Lett.*, vol. 22, no. 10, pp. 694–696, 1997
6. E. Rønnekleiv, M. Ibsen, M. N. Zervas, and R. I. Laming, "Characterization of intensity distribution in symmetric and asymmetric fiber DFB lasers", in *Conf. on Lasers and Electro-Optics*, Vol. 6, 1998 OSA Tech. Digest Series (Optical Society of America, Washington DC, 1998), pp. 80
7. Y. Z. Xu, H. Y. Tam, S. Y. Liu, and M. S. Demokan, "Pump-induced thermal effects in Er-Yb fiber grating DBR lasers," *IEEE Phot. Techn. Lett.*, vol. 10, no. 9, 1253–1255, 1998
8. M. K. Davis, M. J. F. Digonnet, and R. H. Pantell, "Thermal effects in doped fibers", *J. Lightwave Technol.*, vol. 16, no. 6, pp. 1013–1023, 1998
9. W. H. Loh S. D. Butterworth, and W. A. Clarkson, "Efficient distributed feedback erbium-doped germanosilicate fibre laser pumped in the 520 nm band ", *Electron. Lett.*, vol. 32, no. 22, pp. 2088–2089, 1996
10. F. Kreith, *Principles of Heat Transfer*, 2<sup>nd</sup> edition, International Textbook Company, Scranton, Pennsylvania, 1965